

TGV: Tabular Data-Guided Learning of Visual Cardiac Representations

Marta Hasny^{1,2}, Maxime Di Folco^{1,2}, Keno Bressem^{3,4}, Julia Schnabel^{1,2,5}

¹ School of Computation, Information and Technology, Technical University of Munich, Germany

² Institute of Machine Learning for Biomedical Imaging, Helmholtz Munich, Germany

³ German Heart Center Munich, Technical University of Munich, Germany

⁴ Klinikum rechts der Isar, Technical University of Munich, Germany

⁵ School of Biomedical Engineering & Imaging Sciences, King's College London, UK
`marta.hasny@helmholtz-munich.de`

Abstract. Contrastive learning methods in computer vision typically rely on different views of the same image to form pairs. However, in medical imaging, we often seek to compare entire patients with different phenotypes rather than just multiple augmentations of one scan. We propose harnessing clinically relevant tabular data to identify distinct patient phenotypes and form more meaningful pairs in a contrastive learning framework. Our method uses tabular attributes to guide the training of visual representations, without requiring a joint embedding space. We demonstrate its strength using short-axis cardiac MR images and clinical attributes from the UK Biobank, where tabular data helps to more effectively distinguish between patient subgroups. Evaluation on downstream tasks, including fine-tuning and zero-shot prediction of cardiovascular artery diseases and cardiac phenotypes, shows that incorporating tabular data yields stronger visual representations than conventional methods that rely solely on image augmentations or combined image-tabular embeddings. Furthermore, we demonstrate that image encoders trained with tabular guidance are capable of embedding demographic information in their representations, allowing them to use insights from tabular data for unimodal predictions, making them well-suited to real-world medical settings where extensive clinical annotations may not be routinely available at inference time. The code will be available on GitHub.

Keywords: Visual Representations · Contrastive Learning · Cardiac MRI

1 Introduction

Biobanks provide vast quantity of multimodal medical data that can be leveraged to train medical foundation models. Typically, they include tabular data, such as demographic information and medical history, and imaging data, such as MR or CT scans. However, a combination of imaging and tabular modalities has been underexplored compared to the vast research done on image-text models

[18,3]. Meanwhile, in practice physicians often make clinical decisions based on both images and tabular attributes, as information such as patient demographics can provide crucial insights about the patient health. Specifically in cardiology, information such as patient’s sex, age or smoking status are key factors in assessing the risk of cardiovascular diseases [7,1], which is the leading cause of death worldwide [17]. Thus, developing methods that can integrate information from both images and tabular data is crucial for improved clinical decision-making. The curated tabular attributes in biobanks enable the development of novel methods that can leverage this information to train visual encoders capable of embedding tabular information within their representations, allowing them to use those insights even in the absence of extensive tabular data at inference.

One of the paradigms that has been successful in unimodal and multimodal training is contrastive learning [10]. In an image-only setting, contrastive learning typically operates by generating two different views of the same image via augmentations [5], defining them as a pair. In the case of image-text methods, the pairs are formed between corresponding samples of the two modalities to train a joint embedding space [14]. These methods are effective in generalizing across a variety of downstream tasks, often outperforming fully supervised approaches, especially when labeled data is scarce. However, representations trained under those settings often exhibit an issue of false negatives [11,6], as similar samples defined as negative pairs are pushed apart in the representation space. To address this issue in the medical domain, several works have redefined pair sampling strategies. MedCLIP [16] leveraged medical reports to assign soft similarity scores between images and textual descriptions, refining supervision through soft semantic matching. Pai et al. [12] redefined positive and negative pairs in medical imaging by grouping 3D patches containing lesions as positives while treating lesion-free regions as negatives. Hager et al. [8] was the first to integrate medical tabular data and images, combining the settings of SimCLR [5] and CLIP [14] to supervise training of a visual representation using tabular attributes. We extend this work by using the clinical tabular attributes to guide contrastive pair selection for unimodal training, eliminating the need for a joint embedding. Recent studies suggest that unimodal training of medical visual representations can outperform language-based supervision [13], motivating our unimodal approach.

The contributions of this paper are twofold. First, we introduce **Tabular Guide Vision (TGV)**, a novel contrastive learning training paradigm harnessing tabular data to construct clinically meaningful pairs. Rather than enforcing a shared representation between modalities or relying on image augmentations, we use tabular similarity to construct multiple positive and negative pair assignments within images in a unimodal contrastive learning setting. Second, we propose an approach to overcome the limitation of image-only representations, specifically their lack of zero-shot capabilities, by enabling zero-shot prediction within a visual-only setting. Instead of relying on predefined textual prompts, as in an image-text setting, we use a representative sample of images from the training set as a reference. The prediction is then derived as the mean of the tabular attribute values associated with the most similar image embedding in

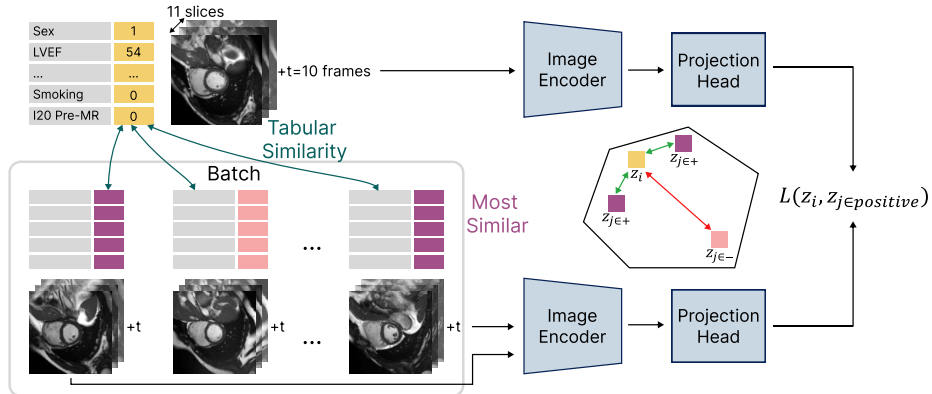


Fig. 1: A schematic view of TGV. In a batch, the image pairs are defined according to their tabular similarity. The loss function is then calculated between the current sample and all its pairs to train a clinically meaningful representation space.

the reference set. We demonstrate the effectiveness of our method by training a visual cardiac representation using MR images and tabular data from the UK Biobank [15] and evaluate it by predicting cardiac health outcomes and phenotype. Our results demonstrate the potential of TGV to leverage multimodal datasets for unimodal prediction.

2 Methodology

The novelty of the method is to leverage a multimodal dataset of image-tabular attribute pairs to learn a representation where clinically similar patients are brought closer in the embedding space, guided by medical tabular data (Fig. 1). We follow the basic setting of SimCLR [5], with a vision encoder E encoding the images into embedding $v \in \mathbb{R}^d$, followed by a projection head f_v mapping the embeddings to $z \in \mathbb{R}^p$, where d and p are the dimensions of the embeddings.

2.1 Defining Similarity Pairs

In a batch of size N , each image x_i is associated with a number of continuous and categorical attributes included in the tabular data $a_i = \{a_{con_i}, a_{cat_i}\}$, which are used to calculate a similarity matrix $S \in \mathbb{R}^{N \times N}$.

Given a matrix of normalized continuous variables $a_{con} \in \mathbb{R}^{N \times M}$, where M is the number of the attributes, we calculate a pairwise Euclidean distance matrix $D \in \mathbb{R}^{N \times N}$. The distance is then converted to a similarity and normalized to match the range of categorical similarity, resulting in a continuous data similarity matrix S_{con} .

Categorical attributes from the batch are represented in a matrix $a_{cat} \in \mathbb{R}^{N \times B}$, where B is the number of categorical attributes in the dataset. Categorical similarity $S_{cat} \in \mathbb{R}^{N \times N}$ is computed via cosine similarity using a_{cat} . The continuous and categorical similarities are then used to calculate the combined similarity between the samples in the batch using:

$$S = \lambda S_{con} + (1 - \lambda) S_{cat}, \quad (1)$$

where λ is a hyperparameter weighting the tabular guidance during the training process towards continuous or categorical attributes.

2.2 Tabular Data-Guided Visual Learning

The constructed tabular similarity matrix S is used to define the training image pairs based on intra-batch similarity. As multiple patients in the batch can be highly similar to each other, an image may have multiple corresponding pairs. For each image x_i in the batch, the most similar image x_j is the one with the highest corresponding similarity score:

$$x_j = \arg \max_{j \neq i} S_{ij}, \text{ for } i, j \in \{1, \dots, N\}. \quad (2)$$

Additionally, a threshold h is introduced such that any other image in the batch with a similarity score within $\max(S_{ij}) - h$ is also considered a valid pair for x_i . This approach ensures that all highly similar instances contribute to the contrastive learning process, leveraging intra-batch relationships. With all the pairs in the batch constructed, the contrastive loss function aligns the representations such that the paired ones are pulled closer to each other, while the unpaired ones are pulled away from one another. The loss is defined as:

$$L = \frac{1}{N} \sum_{i=1}^N -\log \left(\frac{\sum_{j \in \text{positive}} \exp \left(\frac{\langle z_i, z_j \rangle}{\tau} \right)}{\sum_{j=1}^N \exp \left(\frac{\langle z_i, z_j \rangle}{\tau} \right)} \right), \quad (3)$$

where $\langle \cdot, \cdot \rangle$ stands for cosine similarity, τ is a temperature parameter scaling the logits, and $j \in \text{positive}$ defines all the pairs of the given image x_i .

2.3 Zero-Shot Prediction

The setting of our proposed unimodal zero-shot prediction is similar to those presented in image-text joint representation spaces [14]. However, instead of computing similarities between images and text embeddings, we make predictions based on similarities between images in the learned embedding space.

Given a representative sample of images from the training set, i.e., one that captures a range of values for the predicted attribute, we generate representations of those images as a reference set of potential pairings $P = \{v_j | x_j \in \text{training set}\}$.

To make the prediction for an unseen image x_i , the cosine similarity is calculated between its embedding v_i and all embeddings v_j in P , e.g.,

$$s_{ij} = \frac{\langle v_i, v_j \rangle}{\|v_i\| \|v_j\|}, \quad \forall v_j \in P. \quad (4)$$

The prediction for a given tabular attribute a_i is then calculated as the mean of that attribute across the top K most similar images:

$$\hat{a}_i = \frac{1}{K} \sum_{j \in \mathcal{N}_i} a_j, \quad (5)$$

where \mathcal{N}_i is the set of indices corresponding to the K most similar images based on s_{ij} .

3 Experiments

Dataset We use the UK Biobank [15] population study (App. Num. XXX) for the training and evaluation of our method. The dataset contains 49,737 pairs of short-axis cardiac MR and tabular data, out of which 39,975 are used for training, 2,794 for validation, and 6,968 for testing. We use volumes of the cardiac MR as the input to our image encoder consisting of 11 slices over 10 frames, uniformly sampled from the initial 50 frames. The images are zero-padded to a square and then cropped to a size 128x128. Our tabular data consists of 24 attributes, including 10 categorical and 14 continuous variables. The full list of the attributes will be available in our GitHub repository. The continuous attributes consist of the cardiac phenotype, e.g., left and right ventricular ejection fraction. The categorical data consist of demographics information, including sex and smoking, and attributes on the presence of CAD disorders split into those diagnosed pre- and post-MR. The attributes include four different CAD (angina pectoris, acute myocardial infarction, other acute ischaemic heart disease, and chronic ischaemic heart disease) following ICD-10 definition as described by Hager et al. [8]. Due to the low frequency of subjects with CAD, we use a disease-balanced sample for the training of a multi-label CAD prediction comprising 6,426 samples. We only consider diseases reported before the scan date for the classification task. For the fine-tuning of the cardiac phenotype predictions, we use a sample of 5,000 images, with the label quality check performed as described by Bai et al. [2]. Further, a disease-balanced sample of 2,000 patients is included in our reference set P , used for the zero-shot prediction tasks. The zero-shot predictions are based on at most 20% of the most similar embeddings in the reference set for CAD classification and 2.5% for cardiac phenotype prediction. The final percentage is defined by empirical tuning on the validation set.

Implementation All image encoders are 3D ResNet-50 models implemented using the MONAI framework [4]. The embedding dimensions are set to 2048

Table 1: Downstream task performance comparison for multi-label CAD classification (CAD, \uparrow) and cardiac phenotype prediction (remaining columns, \downarrow). ZS stands for zero-shot, FT for fine-tuning, and Aug for image augmentations.

Training	Model	CAD	LVEF	LVEDM	LVEDV	RVEF	RVEDV	MYOESV
-	Mean-Guess	-	4.81	17.85	29.54	4.73	26.73	17.85
Supervised	ResNet50 [9]	65.61	4.31	5.59	10.27	3.81	8.55	6.44
ZS	SimCLR [5]	61.98	4.72	12.92	23.1	4.72	21.67	13.05
	MMCL [8]	61.79	4.4	<u>8.61</u>	<u>15.04</u>	4.48	<u>13.54</u>	<u>9.37</u>
	TGV (w/Aug)	<u>66.6</u>	<u>4.1</u>	10.06	16.26	<u>4.18</u>	15.99	10.43
	TGV (Ours)	67.97	4.08	7.65	13.7	3.98	12.38	8.16
FT	SimCLR [5]	71.68	3.49	5.25	9.82	3.18	8.25	6.06
	MMCL [8]	72.91	3.27	5.63	9.95	3.12	7.75	5.51
	TGV (w/Aug)	<u>75.31</u>	3.11	<u>4.88</u>	<u>9.29</u>	<u>3.03</u>	<u>7.47</u>	<u>5.28</u>
	TGV (Ours)	76.1	<u>3.18</u>	4.86	9.23	2.95	7.39	5.2

for the encoder and 128 for the projection head, following SimCLR [5]. The similarity threshold h is set to 0.05, the regularization parameter λ to 0.5, and the temperature parameter τ to 0.1. The representations are pre-trained for 10 epochs using a batch size of 512 and a learning rate of 1e-3. For downstream tasks, the projection head is removed, and a linear layer is added on top of the image encoder, with an output size corresponding to the number of classes. All downstream tasks are fine-tuned for 35 epochs. For pre-training of MMCL [8] and SimCLR, we follow the original settings described by the authors, with modifications to match the 10-epoch training schedule used by our method.

4 Results

4.1 Representations Strength Comparison

We compare the performance of our method, with and without image augmentations, against a supervised ResNet50 [9] and two self-supervised representation learning methods, image-only SimCLR [5] and image-tabular MMCL [8], across two downstream task categories. First, we report the performance on multi-label CAD prediction using the area under the receiver operating characteristic curve (AUC), as it provides a robust evaluation metric for datasets with a low frequency of non-healthy samples. Second, we evaluate cardiac phenotype prediction using mean absolute error (MAE) across six attributes: left ventricular ejection fraction (LVEF), left ventricular end-diastolic mass (LVEDM), left ventricular end-diastolic volume (LVEDV), right ventricular ejection fraction (RVEF), right ventricular end-diastolic volume (RVEDV), and myocardial end-systolic volume (MYOESV). These attributes are selected to comprehensively assess models’ performance across two characteristic phases of the cardiac cycle

Table 2: Zero-shot demographics prediction. Sex is measured using accuracy, while the other attributes using MAE. The * corresponds to attributes that were not included at pre-training.

	Sex	BMI*	Height*	Weight*
Mean-Guess	-	3.31	7.64	11.78
SimCLR [5]	75.95	<u>2.56</u>	6.2	<u>8.54</u>
MMCL [8]	<u>92.71</u>	2.98	<u>5.12</u>	8.82
TGV (Ours)	98.34	2.31	4.89	7.41

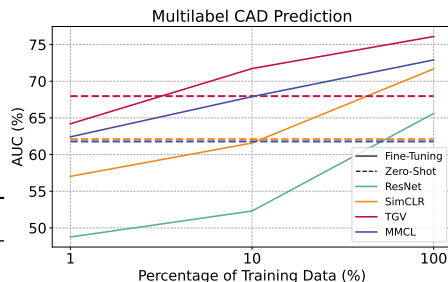


Fig. 2: Performance of the models under low data regime.

and to ensure coverage of the three main anatomical regions of the heart. Table 1 reports the results for both zero-shot prediction and fine-tuning.

TGV without image augmentations (denoted ours in the table) achieves the best performance across all the tasks on both fine-tuning and zero-shot predictions, demonstrating the strength of tabular data guidance in training medical visual representations. This shows that defining clinically meaningful pairs yields stronger representations than image augmentations-based pair sampling. Our comparison of TGV with and without image augmentations shows that not using image augmentations improves the strength of the representation. Further, tabular guidance outperforms tabular supervision, suggesting that training a joint embedding could limit the encoder’s ability to learn directly from the images themselves, due to a strong supervisory signal being provided by the other modality. In contrast, tabular guidance directs the model to learn clinically meaningful information embedded in the tabular attributes directly from the images, resulting in a stronger visual encoder.

Performance under Low-Data Regimes Medical data annotation can be costly and time-consuming. To evaluate the efficiency of the models in low-data regime, we sample 1% (64 samples) and 10% (642 samples) of the original classification training set and use it for fine-tuning. Fig. 2 presents the results of the models fine-tuned with limited data, including a comparison against their performance in a zero-shot setting. TGV achieves the best performance across all data regimes. Moreover, the zero-shot performance of TGV is better than or comparable to the low-data fine-tuning performance of SimCLR [5] and MMCL [8], highlighting the strength of the representations learned by our method.

4.2 Zero-Shot Extraction of Demographic Information

Clinicians commonly use demographic information in their decision making. Thus, it is crucial for an image encoder to capture that information. We perform a zero-shot prediction of four demographic attributes, including sex, weight,

Table 3: Impact of parameter λ (Eq. 1) on the transferability of the method using fine-tuning (FT) and zero-shot (ZS) predictions. $\lambda > 0.5$ increases the importance of continuous attributes in the similarity calculations, while $\lambda < 0.5$ puts more weight on the categorical attributes.

Training	λ	CAD	LVEF	LVEDM	LVEDV	RVEF	RVEDV	MYOESV
ZS	1	62.0	<u>4.36</u>	<u>7.68</u>	<u>12.94</u>	<u>4.24</u>	11.47	<u>8.17</u>
	0.75	64.39	<u>4.36</u>	8.82	14.22	4.4	<u>12.16</u>	9.35
	0.5	67.97	4.08	7.65	13.7	3.98	12.38	8.16
	0.25	65.32	4.52	12.06	19.95	4.57	18.76	12.29
	0	<u>65.44</u>	4.55	11.18	21.46	4.6	20.54	11.4
FT	1	<u>74.05</u>	<u>3.23</u>	<u>5.17</u>	<u>9.57</u>	<u>3.07</u>	<u>7.55</u>	<u>5.39</u>
	0.75	73.83	3.32	5.47	9.74	3.16	7.65	5.59
	0.5	76.1	3.18	4.86	9.23	2.95	7.39	5.2
	0.25	71.39	3.39	5.89	10.28	3.3	7.92	6.19
	0	71.38	3.49	5.98	10.62	3.37	8.11	6.11

height, and body-mass index (BMI). Sex prediction is performed as classification and measured using accuracy, while the other metrics are predicted as a value and evaluated using MAE. Only the sex attribute was included during training, meaning no information about weight, height, or BMI was incorporated to guide the training process. As shown in Table 2, TGV achieved the best performance at capturing the demographics information in its representation space. This suggests that tabular-data guidance allows the encoder to capture information encoded in the image, such as weight or height, even without explicitly incorporating those attributes at training. MMCL [8] outperforms SimCLR [5] in sex and height prediction, while SimCLR achieves better results on BMI and weight. This result further solidifies our claim that tabular data supervision might limit the encoder’s ability to capture information directly from the images by providing a strong supervisory signal in a form of a different modality, reducing the strength of the image encoder itself.

4.3 Impact of Attribute Weighting on the Embedding Transferability

We evaluate the impact of weighting tabular guidance towards categorical or continuous data by experimenting with different values of the hyperparameter λ from Eq. 1. The results are presented in Table 3. The model trained with $\lambda = 0.5$ achieved the best results, outperforming the other models in nearly all zero-shot and all fine-tuning tasks, suggesting that the best performance is achieved when categorical and continuous attributes contribute to the guidance in the same amount. Strong influence of categorical attributes ($\lambda < 0.5$) yields the poorest results. As our dataset has a very small frequency of samples with diseases (8%) and the categorical attributes consist mostly of those describing presence of CAD, there might not be enough variability between the attributes

to properly guide the training. Increased influence of continuous attributes ($\lambda > 0.5$) lowers the performance in comparison to equal guidance, but not as much as strong categorical guidance. This suggests that while continuous attributes retain variability across samples, their differences may not provide sufficiently descriptive signals for tabular guidance.

5 Conclusion

We present TGV, a contrastive learning paradigm leveraging tabular data to generate clinically meaningful pairs for training of visual representations. Our approach outperforms augmentations-based image only contrastive learning and tabular-supervision on CAD classification and cardiac phenotype prediction, highlighting the strength of our approach in a medical setting. Additionally, we propose a zero-shot prediction method compatible with unimodal image representations, overcoming a crucial limitation of those representations. Through zero-shot experiments, we show that our method outperforms previous approaches at capturing demographic information in its representation space. TGV can be leveraged to train medical foundation models grounded on rich clinical information, paving the way for more robust and generalizable medical models.

References

1. Arnett, D.K., Blumenthal, R.S., Albert, M.A., Buroker, A.B., Goldberger, Z.D., Hahn, E.J., Himmelfarb, C.D., Khera, A., Lloyd-Jones, D., McEvoy, J.W., et al.: 2019 acc/aha guideline on the primary prevention of cardiovascular disease: a report of the american college of cardiology/american heart association task force on clinical practice guidelines. *Journal of the American College of cardiology* **74**(10), e177–e232 (2019)
2. Bai, W., Sinclair, M., Tarroni, G., Oktay, O., Rajchl, M., Vaillant, G., Lee, A.M., Aung, N., Lukaschuk, E., Sanghvi, M.M., et al.: Automated cardiovascular magnetic resonance image analysis with fully convolutional networks. *Journal of cardiovascular magnetic resonance* **20**(1), 65 (2018)
3. Bayouh, K., Knani, R., Hamdaoui, F., Mtibaa, A.: A survey on deep multimodal learning for computer vision: advances, trends, applications, and datasets. *The Visual Computer* **38**(8), 2939–2970 (2022)
4. Cardoso, M.J., Li, W., Brown, R., Ma, N., Kerfoot, E., Wang, Y., Murrey, B., Myronenko, A., Zhao, C., Yang, D., et al.: Monai: An open-source framework for deep learning in healthcare. *arXiv preprint arXiv:2211.02701* (2022)
5. Chen, T., Kornblith, S., Norouzi, M., Hinton, G.: A simple framework for contrastive learning of visual representations. In: *International conference on machine learning*. pp. 1597–1607. PMLR (2020)
6. Chen, T.S., Hung, W.C., Tseng, H.Y., Chien, S.Y., Yang, M.H.: Incremental false negative detection for contrastive learning. *arXiv preprint arXiv:2106.03719* (2021)
7. D’Agostino Sr, R.B., Vasan, R.S., Pencina, M.J., Wolf, P.A., Cobain, M., Massaro, J.M., Kannel, W.B.: General cardiovascular risk profile for use in primary care: the framingham heart study. *Circulation* **117**(6), 743–753 (2008)
8. Hager, P., Menten, M.J., Rueckert, D.: Best of both worlds: Multimodal contrastive learning with tabular and imaging data. In: *Proceedings of the IEEE/CVF Conference on Computer Vision and Pattern Recognition*. pp. 23924–23935 (2023)

9. He, K., Zhang, X., Ren, S., Sun, J.: Deep residual learning for image recognition. In: Proceedings of the IEEE conference on computer vision and pattern recognition. pp. 770–778 (2016)
10. Hu, H., Wang, X., Zhang, Y., Chen, Q., Guan, Q.: A comprehensive survey on contrastive learning. *Neurocomputing* p. 128645 (2024)
11. Huynh, T., Kornblith, S., Walter, M.R., Maire, M., Khademi, M.: Boosting contrastive self-supervised learning with false negative cancellation. In: Proceedings of the IEEE/CVF winter conference on applications of computer vision. pp. 2785–2795 (2022)
12. Pai, S., Bontempi, D., Hadzic, I., Prudente, V., Sokač, M., Chaunzwa, T.L., Bernatz, S., Hosny, A., Mak, R.H., Birkbak, N.J., et al.: Foundation model for cancer imaging biomarkers. *Nature machine intelligence* **6**(3), 354–367 (2024)
13. Pérez-García, F., Sharma, H., Bond-Taylor, S., Bouzid, K., Salvatelli, V., Ilse, M., Bannur, S., Castro, D.C., Schwaighofer, A., Lungren, M.P., et al.: Exploring scalable medical image encoders beyond text supervision. *Nature Machine Intelligence* pp. 1–12 (2025)
14. Radford, A., Kim, J.W., Hallacy, C., Ramesh, A., Goh, G., Agarwal, S., Sastry, G., Askell, A., Mishkin, P., Clark, J., et al.: Learning transferable visual models from natural language supervision. In: International conference on machine learning. pp. 8748–8763. PMLR (2021)
15. Sudlow, C., Gallacher, J., Allen, N., Beral, V., Burton, P., Danesh, J., Downey, P., Elliott, P., Green, J., Landray, M., et al.: Uk biobank: an open access resource for identifying the causes of a wide range of complex diseases of middle and old age. *PLoS medicine* **12**(3), e1001779 (2015)
16. Wang, Z., Wu, Z., Agarwal, D., Sun, J.: Medclip: Contrastive learning from unpaired medical images and text. arXiv preprint arXiv:2210.10163 (2022)
17. World Health Organization: Cardiovascular diseases (cvds) (2023), [https://www.who.int/news-room/fact-sheets/detail/cardiovascular-diseases-\(cvds\)](https://www.who.int/news-room/fact-sheets/detail/cardiovascular-diseases-(cvds)), accessed: 2025-02-10
18. Zong, Y., Mac Aodha, O., Hospedales, T.: Self-supervised multimodal learning: A survey. *IEEE Transactions on Pattern Analysis and Machine Intelligence* (2024)